Final Technical Report of Contract ONR N00014-11-1-0521
Entitled:
Low-loss Optical Metamaterials Based on Mie Resonances in Semiconductor Nanoparticle Composites

Submitted by:

Jason Valentine, PI
Mechanical Engineering Department
Vanderbilt University
2301 Vanderbilt Place
PMB 351592
Nashville, TN 37235-1592

December 2012

Abstract

This document is our final technical report and describes the efforts under contract N00014-11-1-0521. The objective of this work was to establish the feasibility of creating solution processed metamaterials formed from composites of semiconductor quantum dots (QDs). The specific goals of this work included, (1) modeling of the metamaterial's optical properties, (2) developing fabrication techniques and (3) experimental characterization of the materials' optical properties. Modeling was first conducted and it was found that under ideal conditions, a high frequency magnetic response could be created in metamaterials formed from composites of quantum dots utilizing excitonic resonances. However, in experimentally fabricated films using cadmium selenide QDs, it was found that the excitonic resonance is significantly broadened, preventing the high index needed to realize metamaterials with tailored effective permittivity and permeability. To overcome this challenge, lead sulfide QDs were then explored due to their high bulk index. Using lead sulfide QDs it was found that a considerably higher effective constituent index could be achieved. However, it was found that thick QD films and multilayer films could not be realized without inducing severe cracking. Patterning of multilayer films was achieved but due to their thin thickness, optical resonances could not be supported.

To overcome the challenges associated with achieving high constituent permittivity and 3D patterning, we have developed silicon (Si) based metamaterials. Using this more conventional material system we have experimentally demonstrated the first zero-index semiconductor based metamaterial at optical frequencies. Formed from stacked Si rod unit cells exhibiting both electric and magnetic dipole Mie resonances, these metamaterials exhibit impedance matched near-zero refractive index at optical frequencies and near unity transmission. The metamaterials possess a nearly isotropic low-index response leading to angular selectivity of transmission through the metamaterial.

REPORT DOCUMENTATION PAGE

Form Approved
OMB No. 0704-0188

1. REPORT DATE *(DD-MM-YYYY)*	2. REPORT TYPE	3. DATES COVERED *(From - To)*
13-12-2012	Final	May 1, 2011 to August 31, 2012

4. TITLE AND SUBTITLE

Low-loss Optical Metamaterials Based on Mie Resonances in Semiconductor Nanoparticle Composites

5a. CONTRACT NUMBER

5b. GRANT NUMBER
N00014-11-1-0521

5c. PROGRAM ELEMENT NUMBER

6. AUTHOR(S)

Valentine, Jason G.

5d. PROJECT NUMBER

5e. TASK NUMBER

5f. WORK UNIT NUMBER

7. PERFORMING ORGANIZATION NAME(S) AND ADDRESS(ES)

VANDERBILT UNIVERSITY
DIVISION OF SPONSORED RESEARCH
BAKER BUILDING SUITE 937
110 21ST AVENUE SOUTH
NASHVILLE, TN 37203-2416

8. PERFORMING ORGANIZATION REPORT NUMBER
4-22-450-3813

9. SPONSORING / MONITORING AGENCY NAME(S) AND ADDRESS(ES)

Office of Naval Research
100 Alabama Street, SW
Suite 4R15
Atlanta, GA 30303-3104 (Lynne Franciosi)

10. SPONSOR/MONITOR'S ACRONYM(S)
ONR

11. SPONSOR/MONITOR'S REPORT NUMBER(S)
n/a

12. DISTRIBUTION / AVAILABILITY STATEMENT

Approved for Public Release

13. SUPPLEMENTARY NOTES

14. ABSTRACT

This document is our final technical report and describes the efforts under contract N00014-11-1-0521. The objective of this work was to establish the feasibility of creating solution processed metamaterials formed from composites of semiconductor quantum dots (QDs). The specific goals of this work included, (1) modeling of the metamaterial's optical properties, (2) developing fabrication techniques and (3) experimental characterization of the materials' optical properties. Modeling was first conducted and it was found that under ideal conditions, a high frequency magnetic response could be created in metamaterials formed from composites of quantum dots utilizing excitonic resonances. However, in experimentally fabricated films using cadmium selenide QDs, it was found that the excitonic resonance is significantly broadened, preventing the high index needed to realize metamaterials with tailored effective permittivity and permeability. To overcome this challenge, lead sulfide QDs were then explored due to their high bulk index. Using lead sulfide QDs it was found that a considerably higher effective constituent index could be achieved. However, it was found that thick QD films and multilayer films could not be realized without inducing severe cracking. Patterning of multilayer films was achieved but due to their thin thickness, optical resonances could not be supported.

15. SUBJECT TERMS

16. SECURITY CLASSIFICATION OF:			17. LIMITATION OF ABSTRACT	18. NUMBER OF PAGES	19a. NAME OF RESPONSIBLE PERSON
unclassified					Valentine, Jason G.
a. REPORT	b. ABSTRACT	c. THIS PAGE	UU	11	19b. TELEPHONE NUMBER *(include area code)*
					615-875-5508

Table of Contents

I. Summary of Accomplishments

This is a final technical report on the work performed under ONR contract N00014-11-1-0521 during the interval of May 2011 through the end of August 2012. The original goal of this contract was to evaluate the feasibility of forming metamaterials from composites of semiconductor quantum dots (QDs). Semiconductor based metamaterials offer the potential advantages of a more isotropic optical response, lower absorption loss, and unit cell architectures that are amenable to 3D scalable manufacturing. Towards this overarching goal, several accomplishments were made including (1) modeling of metamaterials and QD thin films, (2) development of closely packed films of cadmium selenide (CdSe) and lead sulfide (PbS) quantum dots as well as optical characterization of the thin film's optical properties, and (3) successful lithographic patterning of PbS QD films. In the original proposal, the goal was to use the excitonic resonance in CdSe QDs at visible frequencies to realize extremely large constituent permittivity; however, it was found that interactions between QDs in the thin films significantly damped this resonance, making it unsuitable for realizing a high index constituent material. To overcome this issue, focus was shifted to PbS QDs and the telecom frequency range due to the much larger non-resonant permittivity of PbS. Relatively high index PbS QD based thin films were successfully created and they were integrated with a low-index photoresist to create vertically layered unit cells which are necessary for realizing 3D metamaterials. However, difficulties in integration of the photoresist into the QD thin films make patterning of the films difficult. Therefore, while it is possible to create single layer metamaterials using the technique, 3D metamaterials remain elusive.

As an alternative to the above approach, we also investigated semiconductor based metamaterials formed from patterned silicon (Si). This work was begun under the contract that is the subject of this report (N00014-11-1-0521) and is being continued under ONR contract N00014-12-1-0571. In this case, a solid constituent (Si) allows the use of more conventional complementary metal-oxide-semiconductor (CMOS) fabrication techniques, allowing thick 3D metamaterials to be formed. Using the Si material system, we have experimentally demonstrated the first zero-index semiconductor based metamaterial at optical frequencies. Formed from stacked Si rod unit cells exhibiting both electric and magnetic dipole Mie resonances, these metamaterials exhibit impedance matched near-zero refractive index at optical frequencies and near unity transmission. The metamaterials possess a nearly isotropic low-index response leading to angular selectivity of transmission through the metamaterial. These isotropic low-loss metamaterials can be applied for a variety of applications including directional emitters, filters, and compact lens systems.

II. Detailed Descriptions of Accomplishments

1. Modeling of Dielectric Metamaterials

To begin the contract, we examined the electric and magnetic dipole response in unit cells formed from high index constituents. The goal of these studies was to identify the required constituent permittivity which is necessary to avoid diffraction inside the material and ensure a homogenous optical response. These studies were used to establish a target permittivity for the QD composites described below. The optical response of a single layer dielectric metamaterial formed from a constituent with a refractive index of 3.5 is shown in Fig. 1. It can be observed that there is a magnetic dipole resonance at 239 THz and an electric dipole resonance at 294 THz. Also shown is the effective permeability and permittivity of the array calculated using

standard S-parameter extraction [1]. As we approach the first resonance (magnetic) the effective permeability begins to rise at which point a band-gap (BG) is formed due to strong spatial dispersion in the material. This is due to the fact that the effective wavelength inside the material exceeds the lattice periodicity and in this region the effective optical properties have no meaning. As frequency continues to rise, the effective permeability decreases and the wavelength in the material eventually falls below lattice periodicity, allowing homogenization. The same trend is seen at the permittivity resonance. The bandwidth of the spatial dispersion dominated response is a direct reflection of the unit cell size. Furthermore, we have found that as the refractive index of the constituent material drops below 3, the response becomes dominated by spatial dispersion and neither an electric or magnetic metamaterial response can be observed. This agrees with recent calculations described in Peters et. al. [2]. *Therefore, in achieving a metamaterial response with the QD composite constituents described below, it is essential to achieve effective indices greater than 3.*

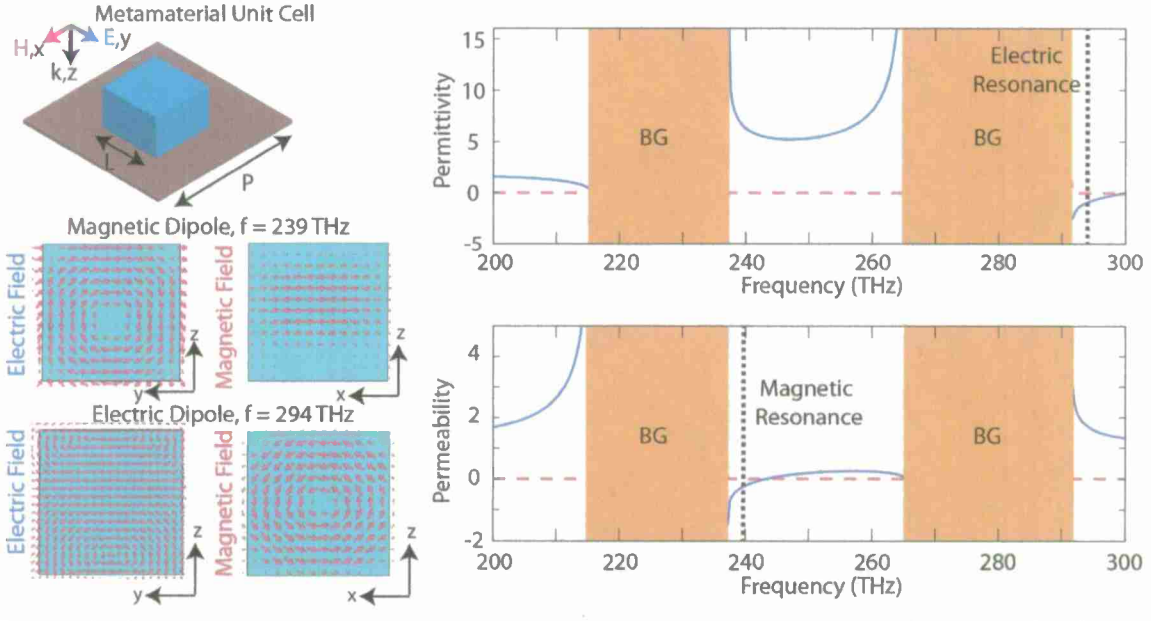

Figure 1. Illustration of metamaterial with a constituent index of 3.5 and extracted effective parameters. The metamaterial has L = 330 nm and P = 660 nm. The magnetic and electric field profiles at the magnetic resonance (f = 239 THz) and electric resonance (f = 294 THz) demonstrate their dipole like field patterns. Areas labeled BG refer to the band-gap of the materials where the response is dominated by spatial dispersion.

2. Modeling and Fabrication of Closely Packed CdSe QD Thin Films

Quantum confinement in semiconductor nanoparticles leads to an increased density of states and a sharp resonance in the permittivity around the lowest absorption band. Our goal was to investigate unit cells formed from tightly packed composites of the QDs to achieve large resonator permittivity at visible wavelengths. In this manner, the composite can be viewed as a meta-metamaterial in which the excitonic resonance in the QD leads to an optical resonance in the larger unit cell (Fig 2a). We originally focused on the use of CdSe QDs as the constituent material in order to achieve an excitonic resonance at a wavelength of ~550 nm and thus a large spike in the permittivity function.

We first theoretically examined the dielectric function of CdSe QD composites near the excitonic resonance. In order to model the dielectric function of the QD films, we utilized an approach developed by Holmstrom et. al. [3]. In this approach, we assume the QD has strong electron confinement and is surrounded by a dielectric shell which can either be a semiconductor or a ligand. The approach also takes into account both linewidth broadening and the size dispersion of the QDs, both important aspects in experimentally realized films. The permittivity of a QD of a particular size and resonance wavelength is then given by,

$$\varepsilon_{QD}^{core-shell}(\omega) = \varepsilon_{\infty}^{core-shell} + [f_c - f_v]\frac{a}{\omega^2 - \omega_0^2 + i2\omega\gamma} \qquad (1)$$

where f_c and f_v are the carrier distribution functions, ω_0 is the resonance frequency, γ is the linewidth, and $\varepsilon_{\infty}^{core-shell}$ is the non-resonant effective index of the core-shell structure. The variable a is given by, $a = 2fe^2 / V_{QD} m_0 \varepsilon_0$, where f is the oscillator strength and V_{QD} is the volume of the QD. It is assumed that the QD's are placed into a matrix with a permittivity of ε_M at a particular filling fraction given by f_{QD}. To take into account size dispersion, we denote the filling fraction of a QD with a particular resonance frequency as f_{ω_0} and use the Maxwell Garnett treatment to find the effective permittivity of the composite by integrating over the resonance frequencies present due to size dispersion. The effective permittivity of the composite is given by,

$$\frac{\varepsilon_{eff}(\omega) - \varepsilon_M}{\varepsilon_{eff}(\omega) + 2\varepsilon_M} = f_{QD} \int f_{\omega_0} \frac{\varepsilon_{QD}(\omega_0, \omega) - \varepsilon_M}{\varepsilon_{QD}(\omega_0, \omega) + 2\varepsilon_M} d\omega_0 \qquad (2)$$

The range of resonance frequencies is calculated by calculating the lowest energy states in the QD's as a function of their size and the size distribution is given by a Gaussian function centered at the nominal size of the QDs.

Theoretical calculations of the permittivity function (Fig. 2b) were conducted for comparison with experimental films (described below). The film permittivity is calculated based on a 68% filling fraction of CdSe QDs with a radius of 2.8 nm and a dielectric shell 1 nm in thickness. Air is chosen as the filler material between the QDs to match the experimental films. The parameters in the model were chosen such that the linewidth of the imaginary part of the permittivity function matches the absorption spectrum of fabricated CdSe QDs measured in solution (not shown). This results in $\gamma = 6$ meV, $f = 4$, and a size dispersion of 5%. The results show that a film with an effective index of 3.5 should be achievable and it should be noted that using a photoresist filler material, instead of air, will further boost the refractive index to close to 4, easily surpassing the goal index of 3.

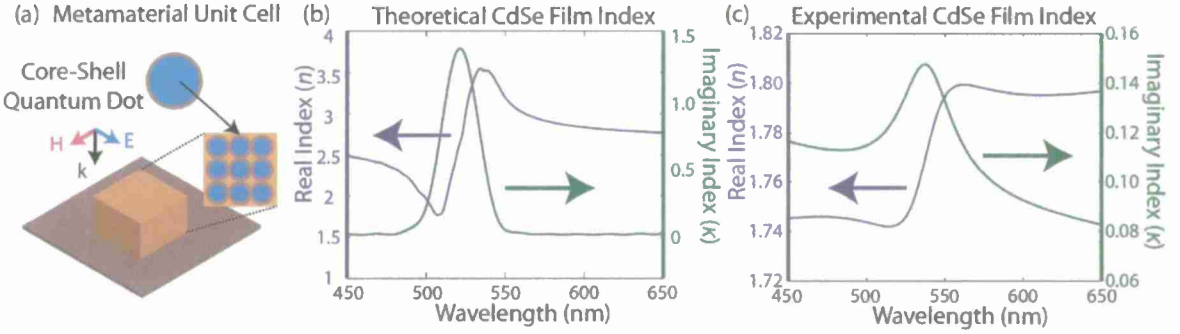

Figure 2. (a) Schematic of metamaterial unit cell comprised of QDs. (b) Theoretical effective index of CdSe QD composite film with 5% size dispersion. (c) Experimentally measured CdSe composite film effective index.

To experimentally realize the films, CdSe QDs were supplied by the Rosenthal group at Vanderbilt. The CdSe QDs were originally functionalized with TOPO ligands and were modified by ligand exchange with shorter MPA ligands to realize higher filling fractions. Ligand exchange occurred during spin coating of the films, resulting in roughly 100 nm thick films with air as the filling material. However, one drawback of this technique is that large cracks form in the film due to the mass loss that occurs in the ligand exchange. These cracks ultimately prevented patterning of the films into unit cells as seen in Fig. 2a.

The refractive index, measured with spectroscopic ellipsometry, of a film of CdSe QDs capped with MPA is shown in Fig. 2c. Based on effective medium modeling outside the resonance, these films have a QD filling fraction of 68%. The maximum effective index achieved was 1.8, far below the goal index of 3. While the absorption linewidth remains sharp in solution, indicating a 5% size dispersion (not shown), closely packed films exhibit significant broadening, leading to a very small resonance in the refractive index. This broadening is most likely due to reduced exciton confinement. We have investigated QDs with varying capping layers including ZnS and ZnSe to increase exciton confinement. However, based on experimental index measurements, we have found that the tradeoff between closely packed quantum dots and resonance peak broadening seems unavoidable. It has come to our attention that this is in fact a central challenge in developing QD based light-emitting diodes and to the best of our knowledge it is only presently avoided by employing single monolayers [4–8], an approach which is unsuitable for the purpose of this work. Ultimately, due to their low index, the CdSe QD films are not suitable for achieving metamaterials with homogenous optical properties.

3. Fabrication and Patterning of PbS QD Thin Films

While it remains a significant challenge to achieve large effective permittivity around the excitonic resonance in the CdSe QD system, a QD material with higher bulk index could be utilized to boost the non-resonant effective permittivity. To explore this option, we investigated PbS QD based meta-metamaterials wherein the *non-resonant* permittivity of the QD composite was used to enable strong unit cell resonances at telecom frequencies. PbS has a substantially higher refractive index (n = 4.22) than CdSe, allowing the composites to approach the permittivity of Si. For instance, PMMA embedded PbS QDs at only a 60% filling fraction should have an effective index of 3.08. It is important to note that this is a non-resonant index and does not require a sharp resonance in the permittivity function due to an excitonic resonance.

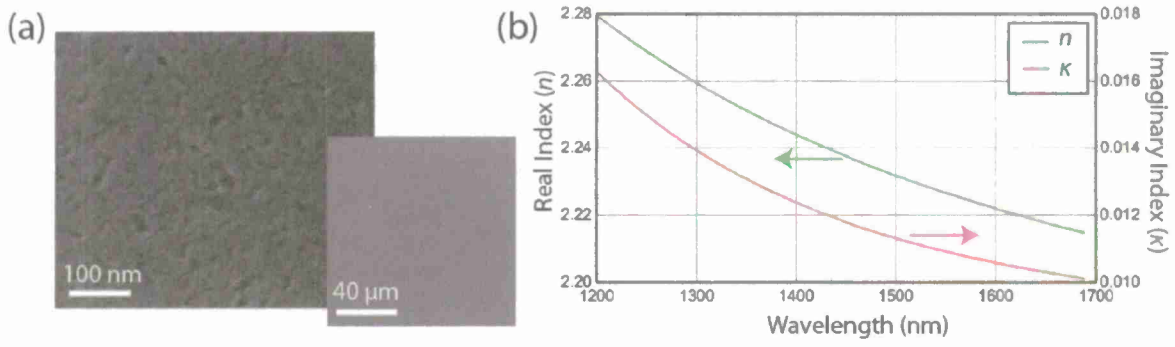

Figure 3. (a) SEM images of PbS QD thin films which are 30 nm after MPA ligand exchange. The films exhibit only minor cracking on a small scale with no evidence of macroscopic crack formation. (b) Index of films measured using spectroscopic ellipsometry.

In order to realize high index films, PbS quantum dots were prepared via colloidal synthesis with an oleic acid ligand. To achieve the highest index possible, the acetic acid ligands were replaced with MPA ligands in an exchange process to enhance the filling fraction of the QDs. To avoid cracking in the film, the MPA ligand exchange was not taken to completion. This was done by first spin coating the QD layer and then immersing the film in an MPA solution for 10 seconds. Replacing the ligands resulted in a significant film thickness reduction from 100 nm to 30 nm. An SEM of an exchanged film is shown in Fig. 3a. One drawback of this method is that generating thick films, on the order of 100 nm in thickness after MPA exchange, always results in cracking due to mass loss. To achieve thicker films, it is possible to perform multiple spins, however, cracks still build up in the films with increasing thickness, making them difficult to pattern. Due to the partial ligand exchange the filling fraction of the QDs was only ~42%, though cracks in the film were largely eliminated. The effective index of the films, measured with spectroscopic ellipsometry is shown in Fig. 3b and has a maximum value of 2.28. While this value is below our goal of an index equal to or greater than 3, there is some room for improvement in optimizing the exchange process. However, before this optimization was performed, we wanted to verify that multilayer films could be accurately patterned, as outlined below.

To evaluate the viability of forming 3D metamaterials, a PbS QD / photoresist multilayer composite was spun onto a wafer in sequential steps (Fig. 4a). Ideally the QD's would be integrated directly into the photoresist layer and then spun onto the films. However, in this case, the volume of the photoresist in the final film prohibits high filing fractions of the QD's and thus should be avoided. To overcome this challenge, separate photoresist and QD thin films were spun sequentially to form the multilayer stack. In this configuration, the goal is to impregnate the QD stack with photoresist spun on top of it in order to pattern the layer. The photoresist that was utilized is hydrogen silsesquioxane (HSQ) due to its short molecule length and thus good permeation into the QD films. HSQ is a negative electron beam resist and has a low refractive index, making it ideal for forming alternating low / high index films. To form materials, HSQ / QD / HSQ stacks were spun then patterned with electron beam lithography. The resulting structures are shown in Fig. 4b and demonstrate that accurate patterning was achieved.

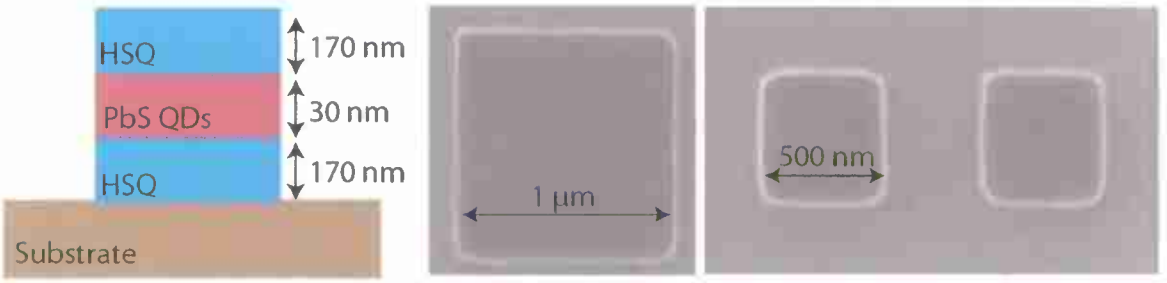

Figure 4. Schematic of multilayer HSQ/PbS QD/HSQ films and patterned films with 1 µm and 500 nm feature sizes, demonstrating the necessary resolution for forming metamaterials from the thin films.

One critical challenge that was encountered is that in QD films thicker than 30 nm, HSQ does not permeate the entire layer, causing the film to peel off the wafer after exposure and development. In QD films thicker than 30 nm, cracking also occurs, making the formation of resonant unit cells difficult. For resonance to occur the thickness of the QD layer must be $\sim\lambda_0/2n$ where n is the effective refractive index of the PbS layer. At a resonant wavelength of 1500 nm, this would require a film thickness of ~330 nm, which seems unattainable using this method for the reasons described above. While these films may find uses for other types of metamaterial and photonic devices, we do not believe it is feasible to realize the original goal of solution processed all-dielectric metamaterials using this method. As such, our attention towards the end of the contract moved towards developing all-dielectric metamaterials using more conventional constituents, as outlined in section 4.

4. Development of Silicon Based Zero-index Metamaterials

While it has proven challenging to realize QD based metamaterials, we have in parallel, developed silicon (Si) based metamaterials. The design of the metamaterial is based off of a recent publication by Chan et. al. [9] where it was shown that through proper arrangement of high index rods in a 2D lattice, an effective index of zero can be achieved. In the work performed under this contract, we have demonstrated how this concept can be scaled to telecom frequencies using stacked Si rod unit cells exhibiting both electric and magnetic dipole Mie resonances. These metamaterials exhibit impedance matched near-zero refractive index at optical frequencies resulting in near unity transmission. The zero-index metamaterial (ZIM) also possesses a nearly isotropic low-index response leading to angular selectivity of transmission through the film. These isotropic low-loss metamaterials can be applied for a variety of applications including directional emitters, filters, and compact lens systems. This work was begun under the contract that is the subject of this report (N00014-11-1-0521) and is being continued under ONR contract N00014-12-1-0571. A journal article is currently under preparation detailing this work.

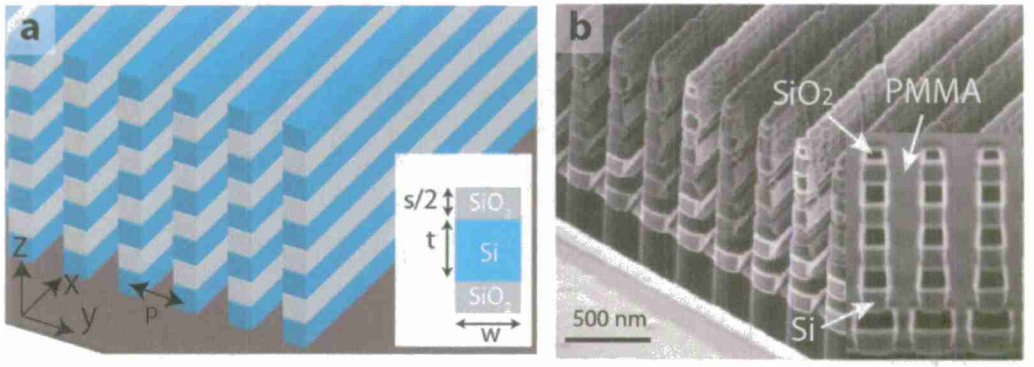

Figure 5. (a) Schematic of ZIM formed from Si rods. (b) SEM image of fabricated structure. The inset shows the structure after filling with PMMA.

A schematic of the fabricated metamaterial is shown in Fig. 5a. The metamaterial consists of infinitely long Si rods separated by silicon oxide (SiO_2). Fabrication was accomplished with conventional CMOS fabrication techniques and can readily be scaled to wafer size using a high resolution optical lithography system. The structure (Fig. 5b) is first patterned using reactive ion etching and then poly(methyl methacrylate) (PMMA) was spun onto the sample to fill the air gaps (inset, Fig. 5b). A total of 5 functional layers (Si / SiO_2 pairs) with a period of a = 600 nm results in a metamaterial with thickness of 3 μm, about twice the free-space wavelength.

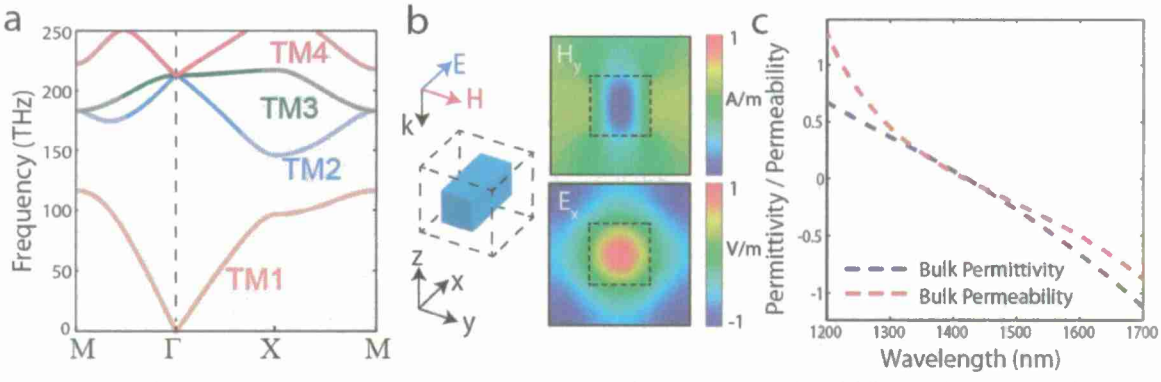

Figure 6. (a) Band structure of metamaterial showing a Dirac point at 220 THz. (b) Electric and magnetic field plots showing the unit cell resonance. (c) Extracted effective material properties of the metamaterial showing an impedance matched zero index at 1400 nm.

The band structure corresponding to the bulk metamaterial (infinitely thick), consisting of a stack of square cross-section Si rods embedded in SiO_2 with $t = w$ = 260 nm, is shown in Fig. 6a. The band structure is computed for transverse magnetic (TM) polarization with the electric field along the rod axis and the Dirac cone dispersion can be observed at the center of Brillouin zone where two transverse bands with linear dispersion intersect a flat longitudinal band, resulting in triple degeneracy. The fields in the unit cells, shown in Fig. 6b, show the strong electric and magnetic resonances which lead to the high frequency magnetic and electric response. We utilized field-averaging to homogenize the structure and retrieve its effective bulk constitutive parameters, illustrated in Fig. 6c. Simultaneous zero-permittivity and permeability are obtained at the Dirac point frequency of ~215 THz, which corresponds to a free space wavelength of 1400 nm. In addition, a relatively broadband low index region is present around the Dirac frequency.

While these bulk parameters are used as a design guide, the fabricated material has both a finite thickness as well as non-uniform rod size and will thus deviate somewhat from the bulk parameters. To determine the experimentally achievable performance, transmittance of the fabricated metamaterials was first acquired by illuminating the sample with normal incident collimated white light with the electric field oriented along the Si rod axis. Figure 7a shows the measured transmittance spectrum along with the numerically calculated transmittance curve obtain from FDTD simulations. The measured spectrum shows a peak of ~80% transmission at 1300 nm which corresponds to the low-index region. The dip in the transmission spectrum at 1400 nm is due to a slight mismatch in the band structure resulting in a small region where the properties are metallic. These regions are confirmed by the extracted optical properties from a metamaterial that matches the actual microstructure (Fig. 7b). While the impedance matched zero-index point is no longer preserved, a low index region extending from 1425 nm to 1380 nm is present and impedance matching occurs when $\varepsilon = \mu = 0.1$.

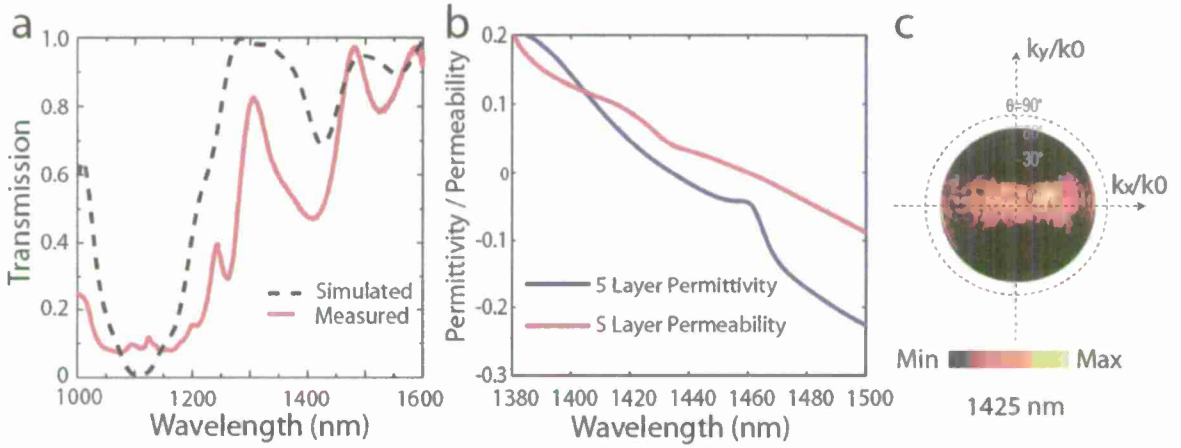

Figure 7. (a) Simulated and measured transmission through the metamaterial. (b) Extracted optical properties from a material matching the fabricated structure. (c) Fourier plane image of light passing through the metamaterial. The incident light is tightly focused. The angle of transmission is strongly confined near 0°.

To experimentally verify the ZIM's isotropic low index and angular transmission selectivity, we obtained the metamaterial's angular transmission pattern through Fourier plane imaging. This was accomplished by focusing a laser beam within the structure using a high numerical aperture (NA=0.85) objective and recording the transmitted Fourier plane image. The angular transmission pattern of the metamaterial at 1425 nm is shown in Fig. 7c demonstrating strong confinement in the y-direction (refer to Fig. 6 for axis direction). It is worth noting that the angular transmission pattern is a line instead of a dot because the angular confinement only works for *k*-vector along the *y*-direction due to the one-dimensional rod structure, namely, the electric field must be along the rod axis to preserve the response. This strong angular confinement is in fact preserved across the entire low index band, though these Fourier plane images are omitted here. This strong angular confinement is a direct reflection of the nearly isotropic low-index response of the metamaterial.

To summarize, we have experimentally demonstrated the first all-dielectric zero-index metamaterial at optical frequencies, exhibiting angular selectivity of transmission. These types of materials may open up new avenues towards the development of optical filters, directional light emitters, and compact lenses. A manuscript detailing this work is currently under preparation and

will be submitted for publication by the end of 2012.

5. References

[1] D. R. Smith, D. C. Vier, T. Koschny, and C. M. Soukoulis, "Electromagnetic parameter retrieval from inhomogeneous metamaterials," *Physical Review E*, vol. 71, no. 3, p. 036617, Mar. 2005.

[2] J. Ginn, I. Brener, D. Peters, J. Wendt, J. Stevens, P. Hines, L. Basilio, L. Warne, J. Ihlefeld, P. Clem, and M. Sinclair, "Realizing Optical Magnetism from Dielectric Metamaterials," *Physical Review Letters*, vol. 108, no. 9, p. 097402–, Feb. 2012.

[3] P. Holmström, L. Thylén, and A. Bratkovsky, "Dielectric function of quantum dots in the strong confinement regime," *Journal of Applied Physics*, vol. 107, no. 6, p. 064307, 2010.

[4] S. Coe, W.-K. Woo, M. Bawendi, and V. Bulović, "Electroluminescence from single monolayers of nanocrystals in molecular organic devices.," *Nature*, vol. 420, no. 6917, pp. 800–803, Jan. 2002.

[5] G. Konstantatos, C. Huang, L. Levina, Z. Lu, and E. H. Sargent, "Efficient Infrared Electroluminescent Devices Using Solution-Processed Colloidal Quantum Dots," *Advanced Functional Materials*, vol. 15, no. 11, pp. 1865–1869, Nov. 2005.

[6] Q. Sun, Y. A. Wang, L. S. Li, D. Wang, T. Zhu, J. Xu, C. Yang, and Y. Li, "Bright, multicoloured light-emitting diodes based on quantum dots," *Nature Photonics*, vol. 1, no. 12, pp. 717–722, Nov. 2007.

[7] K.-S. Cho, E. K. Lee, W.-J. Joo, E. Jang, T.-H. Kim, S. J. Lee, S.-J. Kwon, J. Y. Han, B.-K. Kim, B. L. Choi, and J. M. Kim, "High-performance crosslinked colloidal quantum-dot light-emitting diodes," *Nature Photonics*, vol. 3, no. 6, pp. 341–345, May 2009.

[8] L. Qian, Y. Zheng, J. Xue, and P. H. Holloway, "Stable and efficient quantum-dot light-emitting diodes based on solution-processed multilayer structures," *Nature Photonics*, vol. 5, no. 9, pp. 543–548, Aug. 2011.

[9] X. Huang, Y. Lai, Z. H. Hang, H. Zheng, and C. T. Chan, "Dirac cones induced by accidental degeneracy in photonic crystals and zero-refractive-index materials.," *Nature Materials*, vol. 10, no. 8, pp. 582–586, Jan. 2011.